



Synergistic Effects of Bamboo and Jute Fiber Integration in Geopolymer Composites

P. Gunasekar^{1*}, A. Anderson², S. Saravanakumar³, R. Suresh Kumar⁴, M. Yuvaperiyasamy¹ and K. Sabari¹

¹Department of Mechanical Engineering, Saveetha School of Engineering, Saveetha Institute of Medical and Technical Science, Chennai, TN, India

²Department of Aeronautical Engineering, Sathyabama Institute of Science and Technology, Chennai, TN, India

³Department of Mechanical Engineering, M.Kumarasamy College of Engineering, Karur, TN, India

⁴Center for Advanced Materials & Testing, Department of Mechanical Engineering, Sri Eshwar College of Engineering, Coimbatore, TN, India

Received: 08.05.2024 Accepted: 01.06.2024 Published: 30.06.2024

*konguguna@gmail.com

ABSTRACT

Use natural fiber derived from natural products like fruit leaves, tress constituents, and leftovers can now to create environmentally acceptable materials with excellent mechanical qualities. Geopolymer, on the other hand, behave like materials based on Portland cement in terms of fragility and limited ductility. The assessment of bamboo-reinforcement is the main objective of this work. To investigate the impact of the content of mechanical properties and the type of fiber of resulting composites for geopolymer, varying concentrations of bamboo (ranging from 0.4 to 4.0 wt %) were created. Three-point bending, splitting tensile, and compression testing made up the mechanical characterization process. While one of the mechanical tests bend, ing, which is done by the Point method test, suggested a continuous relation between fiber contented and flexural strength, the outcome of the all-mechanical tests, like tensile and compression tests, demonstrated obtaining the maximum strength of the fiber. Conversely, the compressive, splitting tensile, and flexural strengths of geopolymers with 2% (wt %) bamboo fiber reinforcement increased to 65%, 45%, and 232%, respectively. In all mechanical tests, the inclusion of bamboo fiber at the ideal content causes the samples' failure mode to change from brittle to more ductile.

Keywords: Bamboo fiber; Jute fiber; Geopolymer composite; Tribological properties; Environmental asses.

1. INTRODUCTION

Superior mechanical qualities compared to materials based on Ordinary Portland Cement (OPC) (Cheng *et al.* 2003; Pacheco-Torgal *et al.* 2008; Reig *et al.* 2013a; Atiş *et al.* 2015). For example, Atiş *et al.* (2015) created a fly ash-based mortar for geopolymer that, in just one day, achieved a compressive strength of up to 130 MPa. Using ground granulated furnace slag, (Cheng *et al.* 2003) with creation of geopolymer matrix a first-day compressive strength of 80 MPa. The production of geopolymers based on tungsten mine tailings compressive strength at 27th day which shows strength of 40 MPa was reported by (Pacheco-Torgal *et al.* 2010). Industrial minerals like pozzolan and metakaolin (Mo *et al.* 2014), which have compressive strengths of 65 MPa and 100 MPa on the seventh and 28th days, respectively, have also been used to create high strength geopolymers. Regrettably, matrices of geopolymer have less tensile strengths and brittle attitude, just like other cementitious materials (Sun *et al.* 2008). Regarding cementitious materials, it has been suggested that geopolymers perform better under tensile loads and have better ductility if they are reinforced with both synthetic and natural fibers. The odd infusion of shortened fibers to a cementitious matrix enhances its

fortitude by contribution energy intake mechanisms, ductility by allowing multi-cracking, and strength by transferring stresses across fractures, according to (Arisoy *et al.* 2008). Most studies on fiber-reinforced geopolymers have used fabricated, including basalt fibers (Dias *et al.* 2005; Li *et al.* 2009), fibers made up of steel (Zhao *et al.* 2007), all types of synthetis fibers (Natali *et al.* 2011), fibers which comes from polypropylene (Puertas *et al.* 2003), and fibers which derived from polyvinyl alcohol (Sun *et al.* 2008; Li *et al.* 2009). Natural fiber reinforcing of geopolymer matrices has drawn increased interest recently as environmental concerns about developing novel intensity-effective materials with reduced emissions of carbon dioxide (CO₂) have grown (Silva *et al.* 2010; Yan *et al.* 2012; Correia *et al.* 2013). Correia *et al.* (2013) investigated the use of fibers from bamboo and pineapple leaves to strengthen geopolymers placed on metakaolin in this regard. While comparing to the matrix of unreinforced they discovered that while a 4% (w/v%) fiber content have a detrimental impact on the all strength like tensile and compressive with splitting strength were much higher. By comparing strengths matixs of unreinforced, bamboo fibers raised splitting tensile and flexural strength by 100% and 110 % appropriately. By utilizing additional natural fibers. Sá Ribeiro *et al.* (2016) were

again adequate to enhance the mechanical characteristics of geopolymers based. In their work, a composite material with increased flexural strength (up to 450% more than the control sample) was mixed with 6% (wt%) of water and alkali-studied bamboo fibers and fiber fillet. But when compared the control matrix, the fibers' presence resulted in a roughly 50% reduction in compressive strength, which is comparable to the findings of all fibers (Correia *et al.* 2013). In fly-ash based geopolymer composites. Korniejenko *et al.* (2016) investigated the usage of bamboo fibers at 2% (wt%) and assessed the resulting compressive and flexural strengths. by through comparing unreinforced the results displays that the compressive strength was enhanced by up to 27% by the addition of cotton, bamboo, and coir fibers. Conversely, geopolymer composites with raffia fibers added had reduced compressive strengths. They also observed that the inclusion of fibers like raffia, coir, bamboo and cottons are resulted in 45 % reduction in flexural strength (Chen *et al.* 2014). Through alkali studied sorghum fibers the mechanical characteristics of ash fly base geopolymers are investigated (Alomayri *et al.* 2013; Silva *et al.* 2020a; Thirumalvalavan *et al.* 2023). In this regard, it is estimated that burnt clay brick leftovers make up 30% of the 850 million tons of manufacture and demolition debris that the European Union alone produces annually (Chen *et al.* 2001; Ghosh *et al.* 2016). This study's goals were to assess the use of instinctive fibers like cellulosic, namely bamboo and jute in the formation polymers made from brick fired powder and to examine any potential adverse effects on the mechanical properties that could arise from the fibers' exposure to extremely ALKA surroundings at very young ages and for extended oven-heating times. For this reason, a thorough experimental characterization campaign was conducted. It involved determining the ideal number of fibers to use while taking the mixture's workability into account and analysing the matrices 'feedback to all mechanical strengths later multiple days of manufacturing.

2. MATERIALS AND METHODOLOGY

Though in varying amounts of glucose, hemicellulose, and lignin make up the bulk of both natural fibers. The FAO (Food and Agriculture Organization) views jute and bamboo fibers as future fibers because of it's the advantages they provide to the environment, which is why they were chosen for this study. An acre of jute plants is thought to emit 11 tons of oxygen and absorb roughly 15 tons of CO₂. However, bamboo crops consume higher CO₂, then organic wastes are generated during the manufacturing of bamboo fiber can be used in sectors including the production of fertilizer, animal feed, and bioenergy (Bledzki *et al.* 2015). According to reports, bamboo fibers include 43–56% lignin by weight, 20–25% hemicellulose, and 6–8% cellulose by weight, whereas jute fibers are constituted of 60–65% cellulose, 18–25% hemicellulose, and 11–13%

lignin by weight (Li *et al.* 2000). The density of fibers ranges from 1.30 to 1.45 g/cm³, but the density of bamboo fibers is approximately 1.45 g/cm³ (Dhinakarraj *et al.* 2023). Both fibers are sliced in to geometric length of 10 mm for the purposes of this investigation from commercial products (ropes), yielding the attitude of proportion of 190 and 75, subsequently. Scanning electron microscopy was used to examine the longitudinal and cross-sectional morphologies of both fibers. The findings are shown in Fig. 1. According to longitudinal micrographs (see Figs. 1a and b), bamboo fibers have tough surfaces than jute fibers, which may improve the fiber's adherence to the geopolymer matrix. All fibers should made up of cells which is derived from linked fibers, substance that resembles adhesive, as seen in Fig. 1 (Phologolo *et al.* 2012).

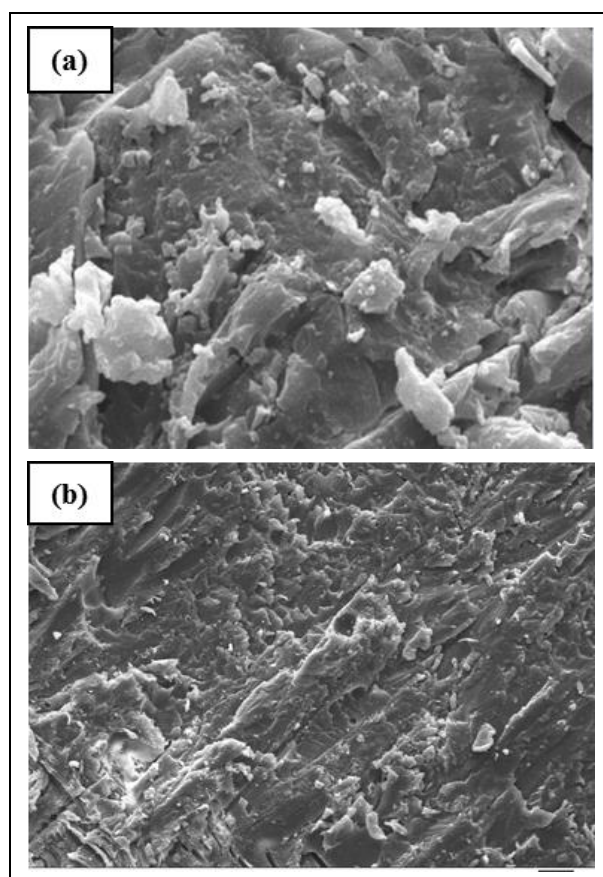


Fig. 1: SEM images of natural fibres which is used for reinforcement geopolymer matrix based on FCBP (a) Jute fibre longitudinal view (b) Bamboo fibre longitudinal view

Water consumption and water influence intersection experiments were performed on bamboo and jute fibers to find out how wettable they were. Before the experiments, both fibers were dried for 24 hours at 65 degrees Celsius. Water absorption and water contact angle experiments were performed on bamboo and jute fibers to find out how wettable they were. Prior to the experiments, both fibers were dried for 24 hours at 65 °C. The fibers were dried and then wrapped in water for a

whole day to assess water consumption. The fibers were then able to achieve a saturated surface dry state (SSD) after the extra water was removed from their surface using absorbent paper. Equation (1) was used to measure the water consumption quantity (A), here w and d represent mass of the fibres under non wet circumstances and at the SSD, appropriately.

$$\text{Absorption of water (A), \%} = ((w-d)/d) * 100 \quad (1)$$

In contrast, a glass slide was used for influence angle testing, and several fibres were arranged and arranged together to make a horizontal exterior that was roughly 1.6 mm broad. The flattened group of fibers was studied with an individual droplet of distilled water (0.5 mL), and after 1, 10, 20, and 30 s, the connection angle was studied with a Ramé-hart contact angle goniometer. According to the water absorption test findings, bamboo and jute fibers had values of $125\% \pm 5\%$ and $102\% \pm 13\%$, respectively. This suggests that bamboo has a

higher water consumption scope than jute. Additionally, experiments use water as connection angles (Fig. 2) show that bamboo fibers are noticeably higher hydrophilic than jute fibres. Even after being exposed to the water droplet for 30 seconds, jute fibers still had a connection angle of 70° . Conversely, after 1 second of exposure, bamboo fibers showed a lower initial connection angle of 45° , which quickly reduced. The water drop was absorbed by the material ten seconds after it was set, making it impossible to determine the contact angle (Fig. 2j). According to these findings, bamboo fibers have a higher affinity for water than jute fibers, which is important for forming a strong and positive contact betwixt the fiber and the water-based geopolymer matrix (Ranjbar *et al.* 2016). Using Mts machine with capacity of 5 kN the tensile test is analysed and a 6 mm/min moves rate were used to examine the tensile strengths of bamboo and jute fibers.

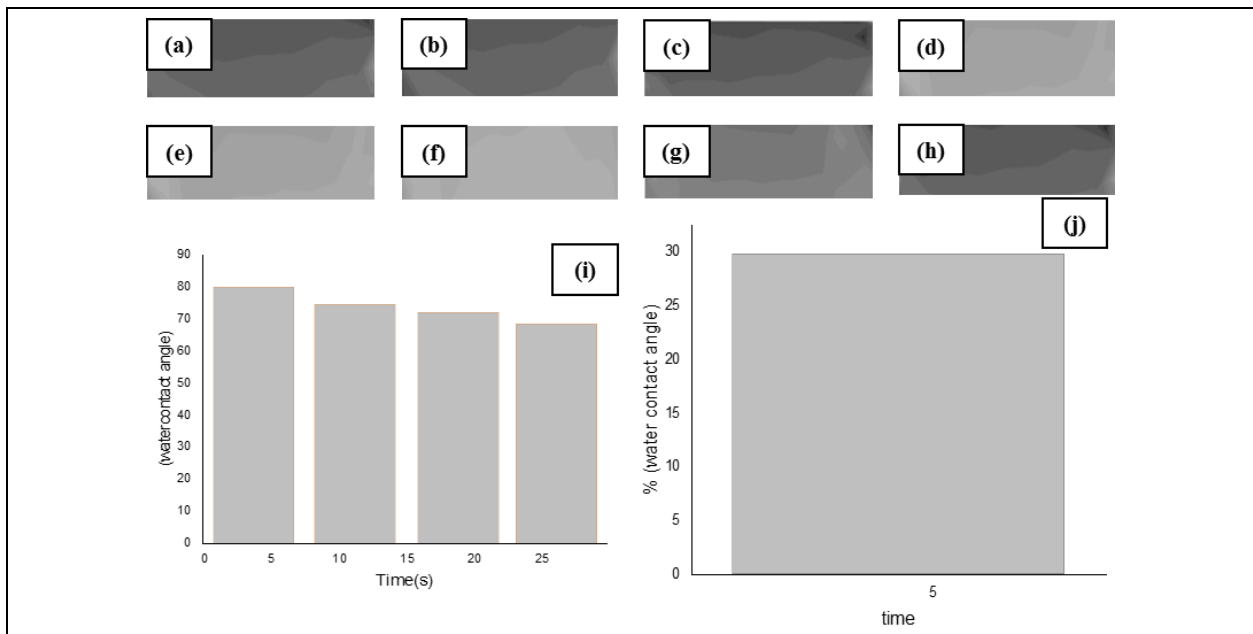


Fig. 2: Fibre test conduct for water contacts and time variation for jute and bamboo

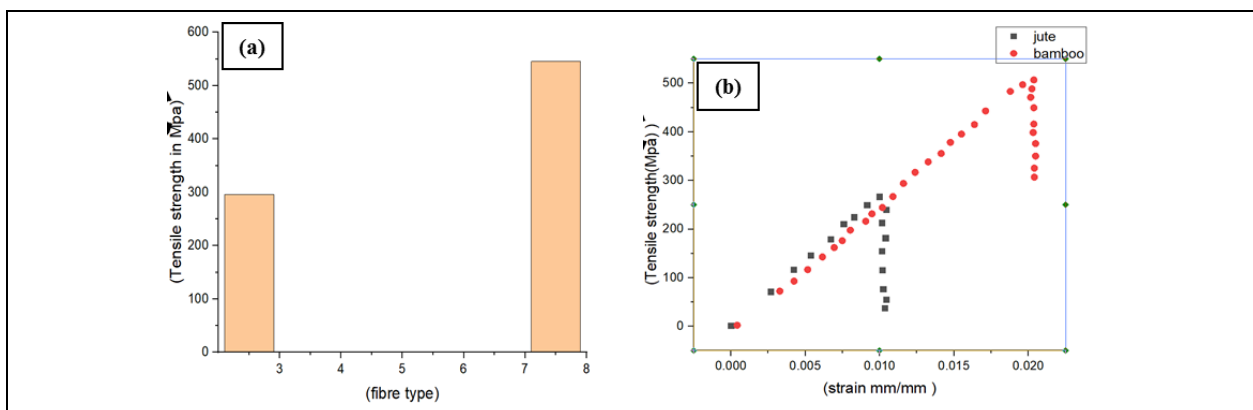


Fig. 3: Individual jute and bamboo fibres: (a) Tensile strength (b) Tensile stress vs strain

Tensile testing on single fibers were carried out in accordance with ASTM D3822 criteria (Silva *et al.* 2020b). The scale of the enforced load to the fiber's moderate transversal area was used to compute the tensile stresses. To create the all-comparative curves like strain and stress, the ratio between the grasp distance and the crosshead displacements was measured. The tensile strength tests for both types of fiber are displayed in Fig. 3a. Six exhibit of all kind of fiber were analysed. It can be shown that bamboo fibers has tensile strength of 508 MPa, whilst jute fibers had a strength of 276 MPa. Fig. 3b shows the tensile stress vs. strain curves for all fibers. Even though their tensile strengths differ, it is evident. Jute fibers had an E-modulus of 28 GPa, whilst bamboo

had little low rate of 26 GPa. But as Fig. 3b illustrates, bamboo fibers conferred 98% higher prolongation quantity than jute fibers. The raw material's reactivity may be enhanced by the FCBP, which produced an average particle diameter of 17.15 μm (Fig. 4a). The SEM micrograph of FCBP that is displayed in fig 4b demonstrates actual irregular and crystal-like form morphology. The FCBP's chemical composition refer table 1 with higher concentration of SiO_2 , Al_2O_3 , and Fe_2O_3 , was shown by X-ray fluorescence analysis, confirming the right conditions for the creation of geopolymers. Further details about the microscopic and mineralogical analysis of the FCBP used in this work (Silva *et al.* 2019).

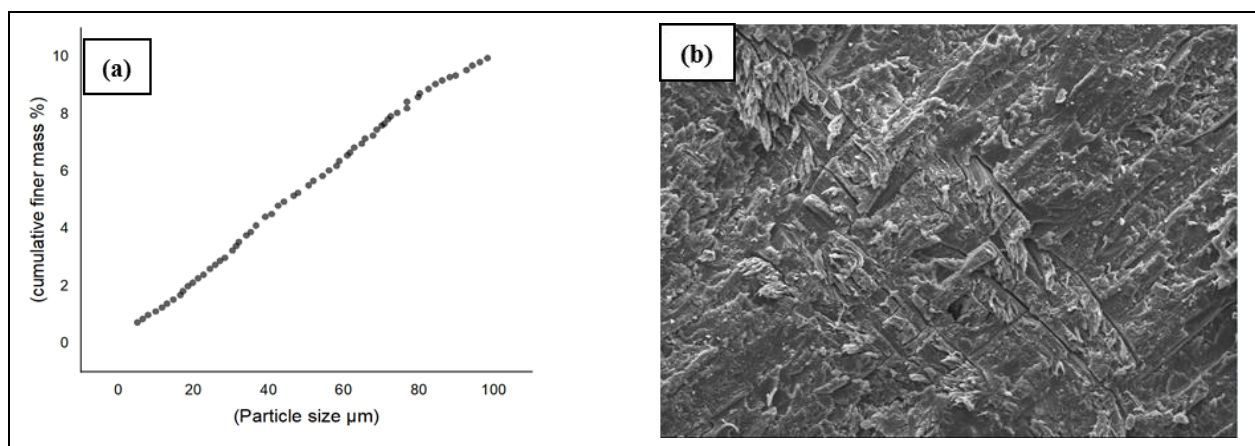


Fig. 4: Particle size distribution and analysis of FCBP: (a) Casing curves (b) SEM graph

Table 1. Point out FCBP composition of chemical by method of XRF

Oxide content (w/w %)							
SiO_2	Al_2O_3	Fe_2O_3	K_2O	MgO	CaO	Na_2O	other
52.45	19.85	8.10	2.64	1.86	1.52	1.29	10.43

The raw material's potential reactivity may be enhanced by the FCBP, as evidenced by the average diameter magnitude of 18.15 μm (Fig. 4). The form morphology of FCBP is remarkably like a crystal, as seen in the SEM micrograph shown in Fig. 4. The FCBP's X-ray fluorescence examination revealed a chemical composition (refer table1) with an immense concentration of SiO_2 , Al_2O_3 , and Fe_2O_3 , confirming the right conditions of geopolymer synthesis. Refer to (Silva *et al.* 2019) for further details Fig. 6 shows optical image done by microscopic level for geopolymer composites, on the microscopic examination of the FCBP used in this study. A sodium silicate solution, purified water, and NaOH pearls (99% weight and purity) were combined to create the alkaline activating solution. By substance, the sodium silicate solution is composed of 28% SiO_2 , 8% Na_2O , and 64% H_2O .

2.1. Steps for experimental

As per ASTM C1437-15, flow tests were conducted on newly created FCBP-based geopolymer composites to examine the impact of jute and bamboo fiber content on the mixture's workability. To do this, the fresh material was evenly divided into two coating and compressed by tamping all layer 20 times in a truncated conical Mold with dimensions of 70 mm for the upper diameter, 100 mm for the bottom diameter, and 50 mm for the highness. Following a minute, the Mold and material setting was taken out for multiple drops more than 25 times. According to the protocols outlined in ASTM 109 (Ramu *et al.* 2023), ASTM C496 and ASTM C348 (Deepanraj *et al.* 2023) carried out to assess the impact of the addition of jute and bamboo fibers on the mechanical properties of FCBP-based geopolymer

composites. For all mechanical tests of geopolymer composites, an electromechanical testing apparatus MTS exceed 45.105 (Fig. 5a) with a 100 kN capacity was employed. For every mechanical test, the global displacements that matched the load frame's displacements were recorded. The load frame's displacement rate was set at 0.5 mm/min. For compression tests, 50 mm-side cubic samples were used (see Fig. 5b); for splitting tests, cylindrical specimens with 40 mm in diameter and 80 mm in height were used (see Fig. 5c); and for three-point bending tests, prismatic samples with approximate dimensions of 40 mm ~ 40 mm (cross-section) ~ 160 mm (length) were used (Fig. 5d). The distribution and interactions between the bamboo and jute fibers inside the binder mixture were examined using SEM. With an operating voltage of 30 kV, all SEM imaging of fiber-reinforced fractured samples was carried out by an FEI Quanta 200 SEM. Since additional water addition has been shown in prior research to reduce the mechanical characteristics of geopolymer matrices, the idea of adding more water to offset the workability loss caused by fibers was not taken into consideration (Reig *et al.* 2013b). The geopolymer mixes were poured into cubic, cylindrical, and prismatic silicon Molds, and the air bubbles were removed by vibrating the Molds. Samples were demoulded after 24 hours but were maintained in the oven while the specimens were cured for three days at 65 degrees Celsius. After that, the specimens were stored at room

temperature for four more days till mechanical testing were done. To prevent the fibers in FRGC from deteriorating, the oven curing period was restricted to three days.

The authors of (Silva *et al.* 2019) show that because FCBP-based geopolymers require relatively high temperatures during the first phase of formation, curing at room temperature was ignored. An overview of the FRGCs' preparation and curing conditions is included in Table 2, along with the quantity of tested samples used in the mechanical tests.

3. RESULTS AND DISCUSSION

The impact of bamboo and jute fiber incorporation on workability of geopolymer composites - as determined by the mixes' flowability is depicted in Fig. 7. Equation (2) was used to calculate the flowability (F), which is the relative difference between the tested matrix's (D) average base diameter and the Mold bottom diameter. The findings displayed in Figure 7b suggest that there is a direct correlation between the fiber content and flowability of both FRGCs. On the other hand, bamboo-FRGCs showed a smaller decrease in workability for the same fiber percentage. For instance, bamboo-FRGC had a 50% greater flow capacity than jute-FRGC at a 2% fiber content (Do).

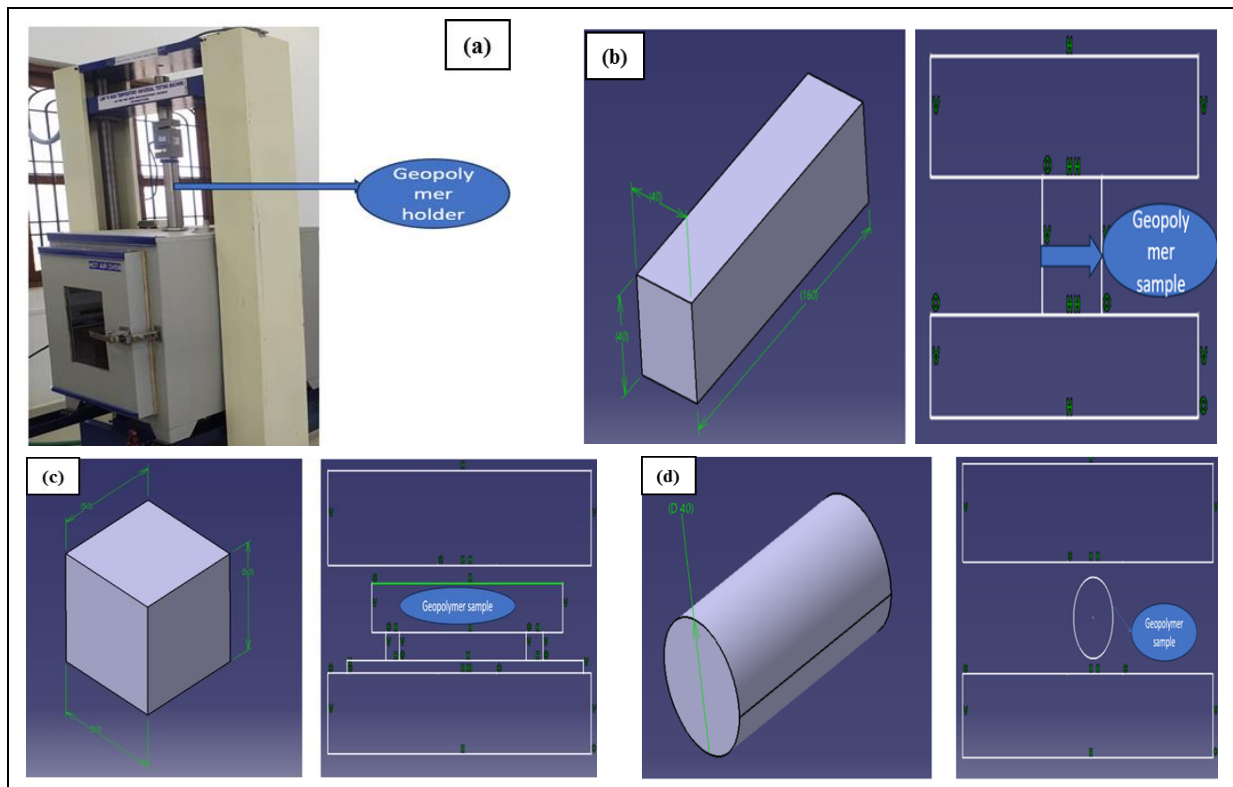


Fig. 5: (a) UTM (b) Geopolymer cupe sample (c) Geopolymer cylindrical sample (d) Prismatic sample and tensile testing test (units in mm)

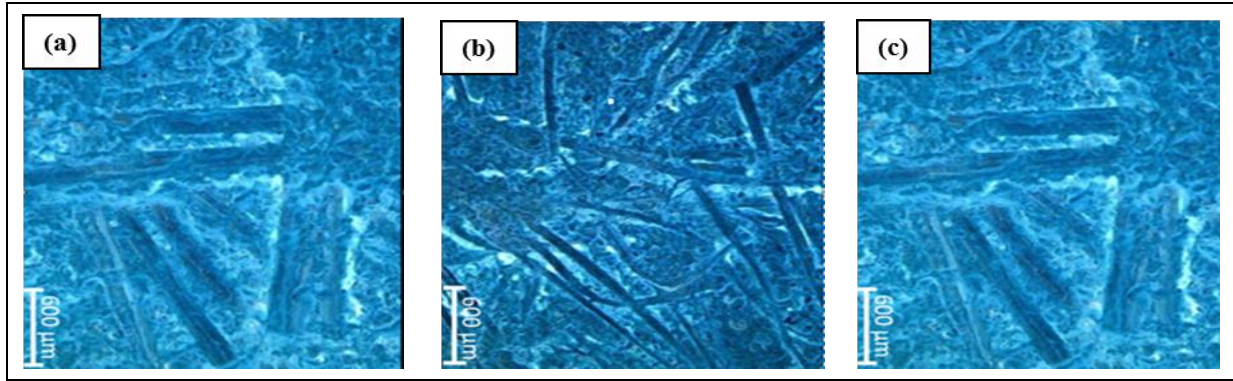


Fig. 6: Signals images for optical microscope of geopolymer composites: (a) Control matrix; (b) Jute FRGC; (c) Bamboo FRGC

Table 2. Summaries of curing and testing condition of tested samples (FRGC)

Type of fibre	Fibre addition wt. %	Sampling tests	Millimoles per mole	Na ₂ O (wt. %)	Water/binder wt./wt.	Time and curative temp	Curing fixes up total
Control grid	-	8	0.558	7.98	0.28	3 days and 70 °C	7 days
Jute	0.49	8	0.60	8	0.27	3 d and 70 °C	7 d
	1.00	8					
	1.50	8					
	2.00	8					
Bamboo	0.50	8	0.60	8	0.27	3 d and 70 °C	7 d
	1.00	8					
	1.50	8					
	2.00	8					
	2.50	8					
	3.00	8					

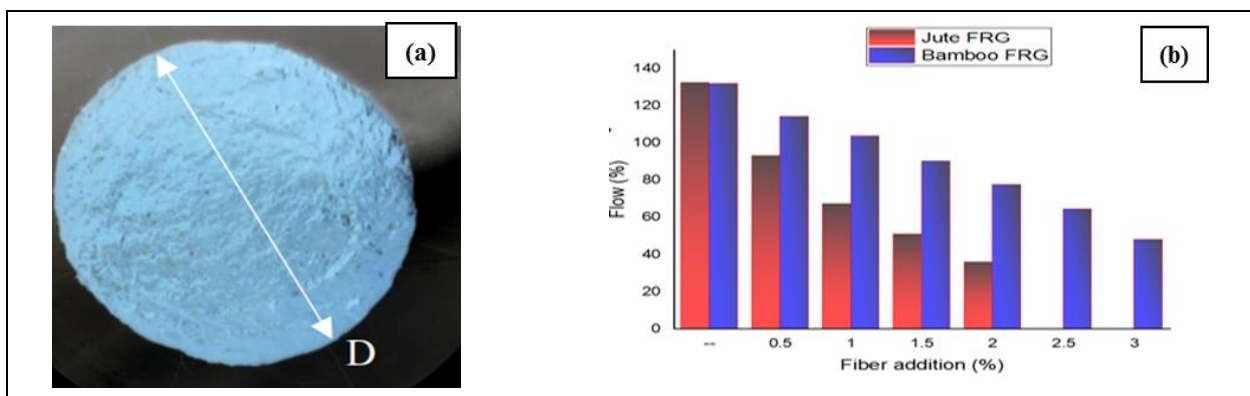


Fig. 7: Illustrate FRGC flow tests: (a) FRGC flow setup; (b) Results for flowability of jute and bamboo fibres

As observed by (Yazici *et al.* 2007), to who noted reinforced materials workability reduces as the attitude proportion grows, that can be due to the diminished attitude ratio offered by bamboo fibers. This test made it possible to determine the maximum percentages of bamboo (3%), and jute (2%) that could be added to the combinations.

$$F = S = ((S - S_0) / 100) \tag{2}$$

Complex that it was not possible to analyse a higher amount of fiber. The results of reinforced bamboo

and jute fibers with FRFCs, appropriately are displayed in Fig. 8a and 8b. Fig. 8 demonstrates here is a particular amount of fiber gratified that magnify the bulk density (2 % of all bamboo FRGC and jute in contrast to other research that reveal an inversely comparable relation between the bulk density and the fiber contented (Alomayri *et al.* 2013; Chen *et al.* 2014; Ranjbar *et al.* 2016). This study differs significantly from earlier publications because no additional water was supplied to make up for the workability that was lost when fibers were introduced. Large amounts of intergranular holes would form in the microstructure because of an inevitable

inclusion of additional water to the blend and its consecutive dispersal during curing, which would lower the bulk density of the composites (Alomayri *et al.* 2013). Higher manufacturing compaction owing to workability loss and increased fresh mixture viscosity from fiber

addition can account for the initial density gain observed in both FRGCs relative to the regulation matrix. Nonetheless, the bulk density of both FRGCs decreases as the fiber content exceeds 1% (wt.).

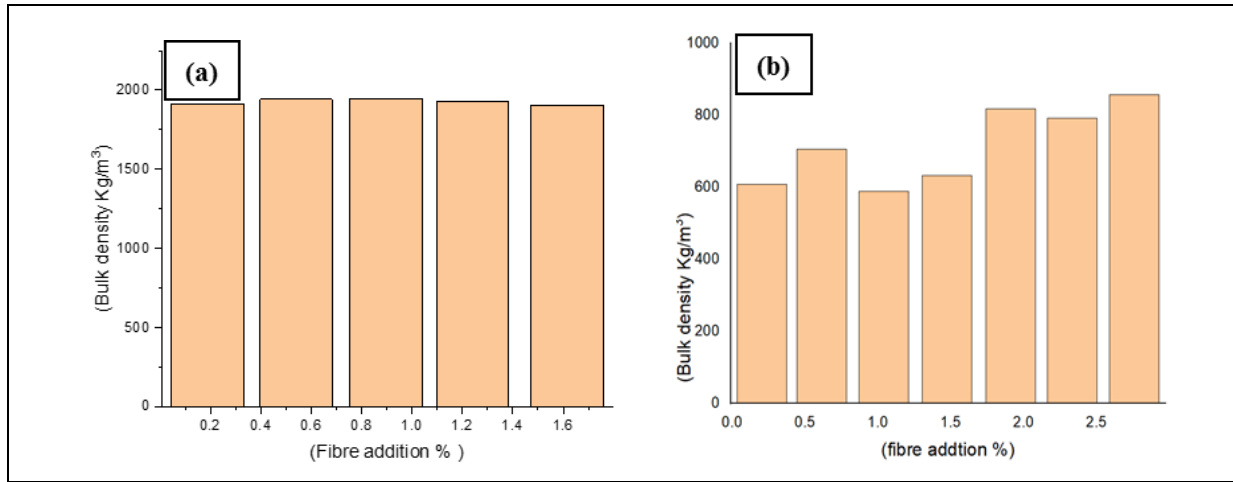


Fig. 8: Mean geopolymer composites test results (a) Jute fibers; (b) Bamboo fibers

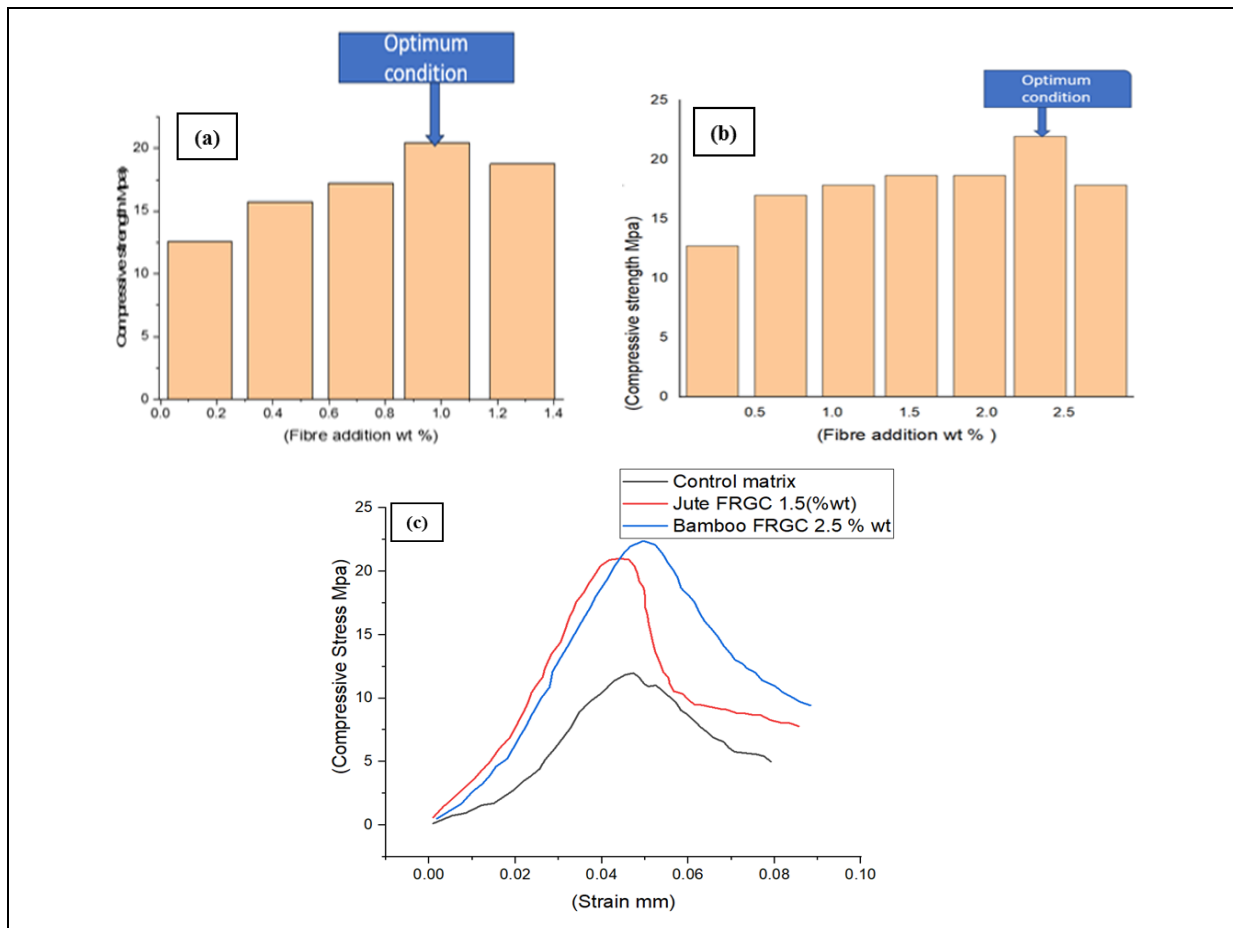


Fig. 9: Demonstrate geopolymer reinforced compression test results: (A) Jute reinforced; (B) Bamboo reinforced; (C) compression Vs Strain curves

Even with increased compaction energy used during manufacture, there may be a loss of bulk density due to fiber agglomeration during mixing at high fiber concentrations. Intergranular holes created by fiber agglomeration in composites may potentially be detrimental to the materials' mechanical qualities (Alomayri *et al.* 2013). The outcomes of the compressive analysis for uniaxial conducted on the FRGCs and control samples are displayed in Fig. 9. The geopolymer composite compression strength behave better than the control sample, as seen in Fig. 9a and 9b. Furthermore, the data show a tendency toward increased strength with increasing fiber content, up to a point where decline is seen, that the kind of fiber determines the maximum strength. When the fiber content was 1.5% (wt%) in the

instance FRGC jute seventh day compression strength captured maximum of 21.02 MPa of indicating a 64% improvement over the control. However, when correlated to the control matrix, bamboo-FRGC specimen with 2.8 percentage of weight fibers showed the largest enhancement (78%) on the seventh day reaching 22.1 MPa. For both varieties of FRGC, higher fiber concentrations resulted in a drop in compressive strength. Fig. 9c displays control matrix of the compression stress strain curves, the ideal jute -FRGC (containing 2.0 WT % fiber), and bamboo FRGC (2.5wt % fiber). Both the jute and bamboo-FRGCs show higher E-moduli (103% for jute and 76% for bamboo) when correlated to the control matrix.

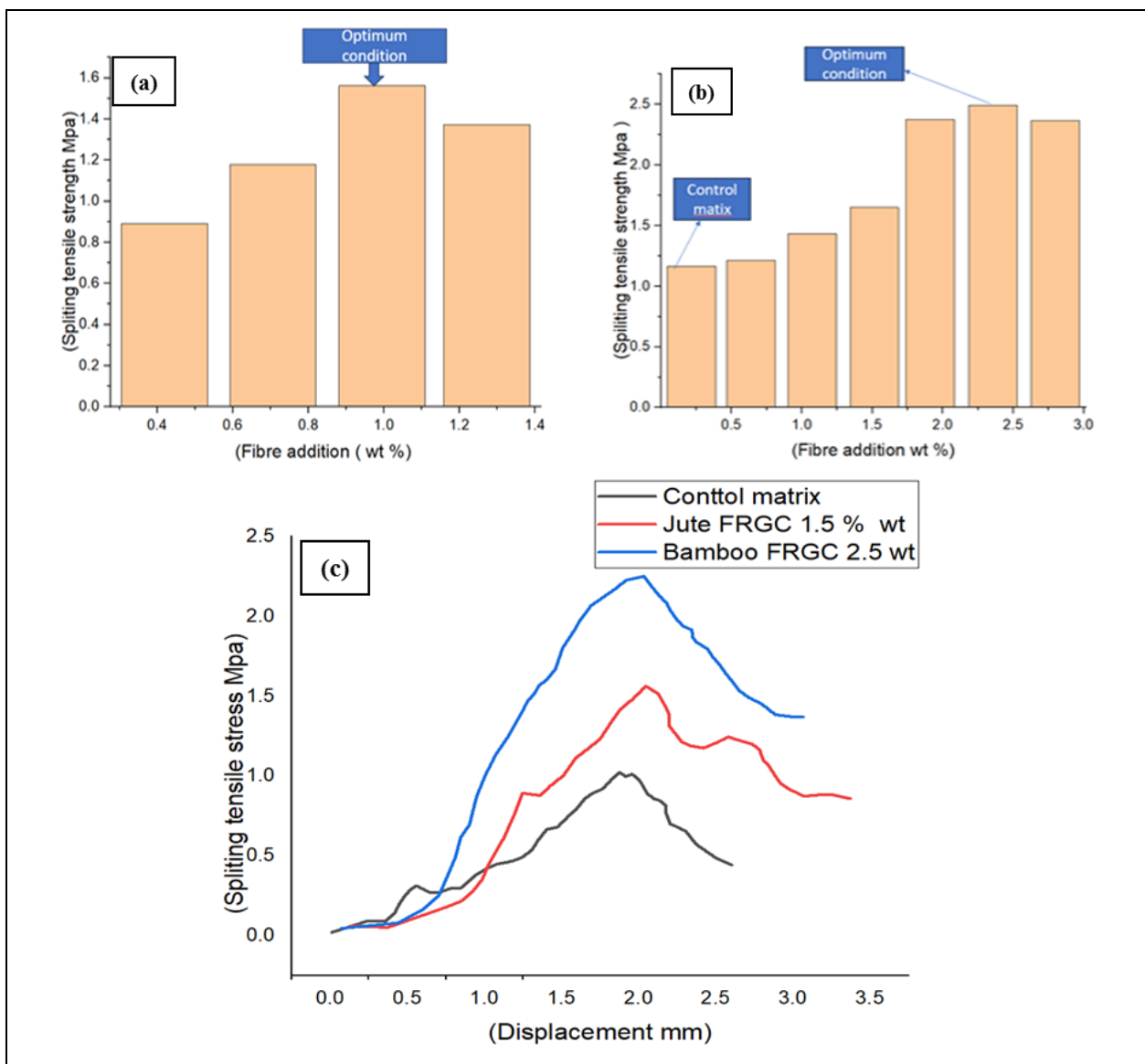


Fig. 10: Reveals test results for splitting analysis: (a) With jute splitting test results; (b) Bamboo reinforced with splitting test results; (c) Tensile strength stress versus displacement curves

During the compression tests, the existence of all fibers considerably altered how sampling in pieces apart. A control matrix (no fiber reinforcement) exhibits a brittle failure mode in Fig. 9d, with the production of tiny free pieces. However, it is evident from the modes of failure of FRGCs containing bamboo and jute fibers that they exhibit a more ductile nature Figure 10 displays the splitting test results. It is evident that the tested matrices behaved better under tensile loads when bamboo and jute fibers were included. Both FRGCs demonstrated the increment in fiber content up to an optimal standard, which is consistent with what was shown in compression tests. The inclusion of 2.0% (wt.%) of fibers to FRGC jute produced maximum value of tensile strength (1.7 MPa) surpassing control matrix's strength by 45%. This is the same optimal value found in the compression testing. With 2.5% (wt.%) more fiber added, the tensile strength of FRGCs expanded to 2.4 MPa (114%) greater than the control matrix), which is also optimal value

found in the compression testing. When compared to the FRGCs control matrix, with the ideal fiber content again showed improved tensile toughness (see Fig. 10c). The range under the displacement curve vs splitting tensile stress represents the tensile toughness. Comparing 2.5 % bamboo FRGC AND 2.0 % jute FRGC to the control matrix, the tensile toughness of the two samples increased by 92% and 181%, respectively. Lastly, higher failure mode of ductile was revealed by FRGC splitting test when compared to the control grids (see figs 10). Therefore, fibers permit payload transmission from the fractured location to alternative flawless segment of the sample, FRGCs exhibit multi-cracking fracture behaviour. These findings concur with those of previous writers (Sun *et al.* 2008; Chen *et al.* 2014) who described how the inclusion of short fibers causes fly ash-based geopolymer matrices to change from having brittle to ductile behaviour.

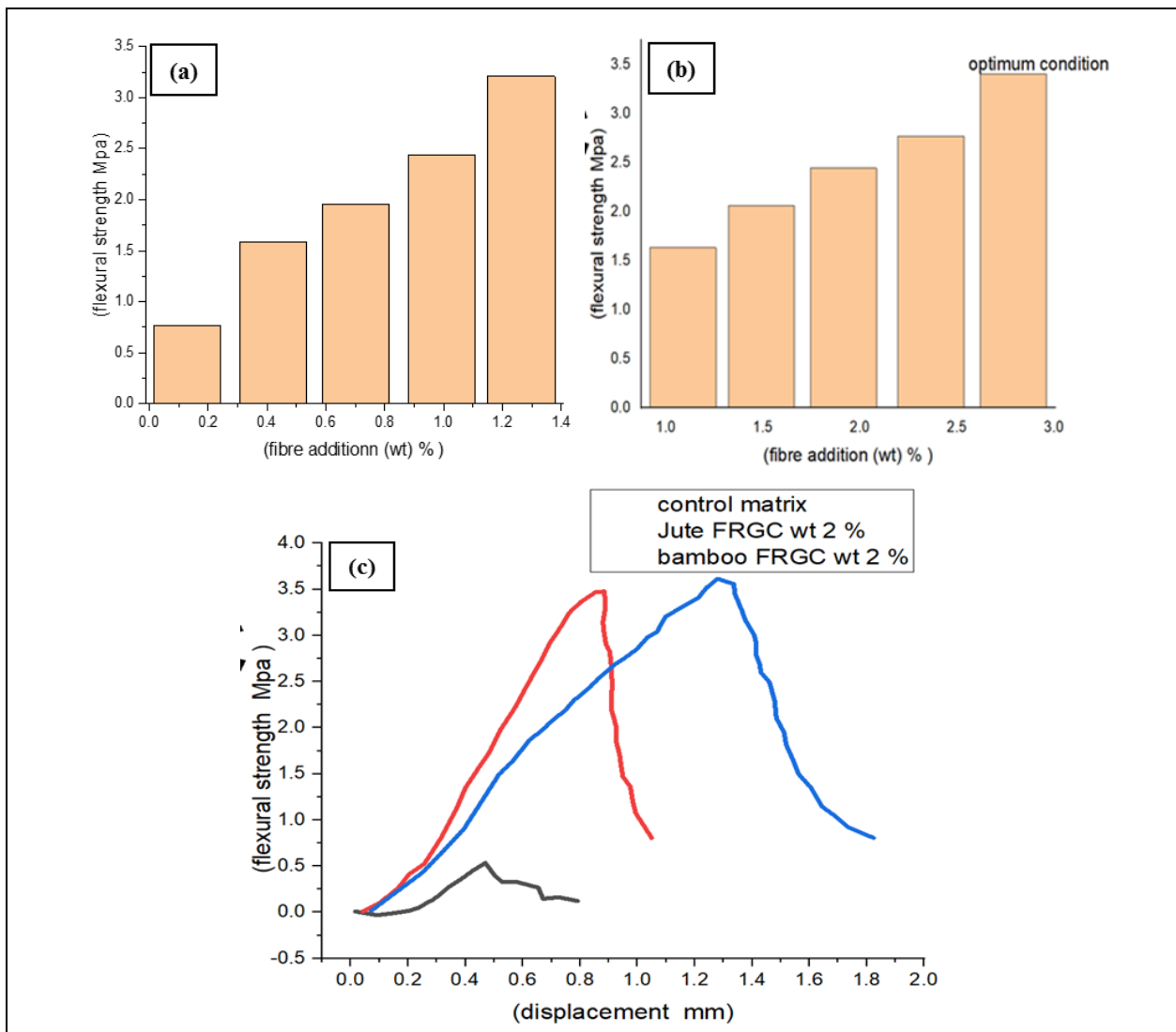


Fig. 11: Pinpoint geopolymer testing analysis by three-point bending method: (a) for jute with reinforced; (b) for bamboo fibers; (c) flexural strength stress versus displacement curves

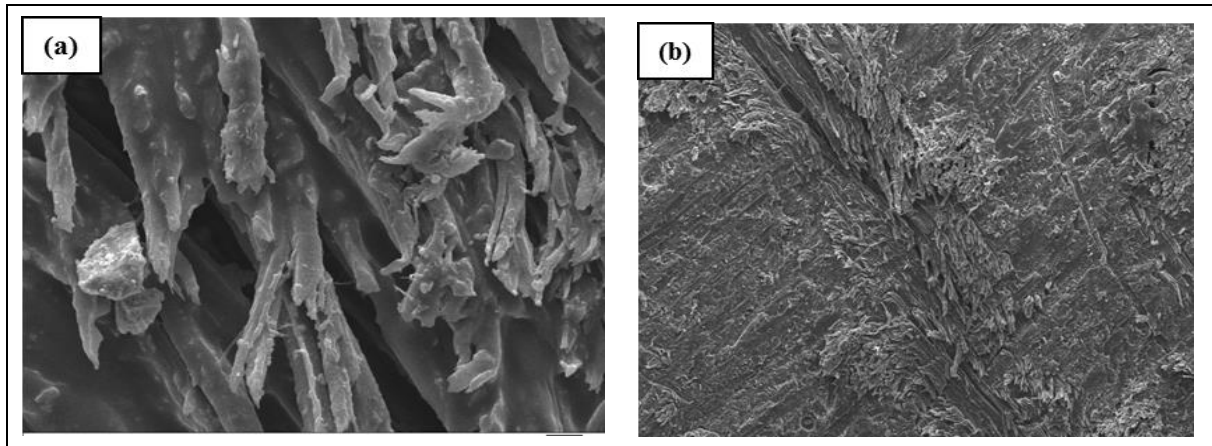


Fig. 12: Cracked FRGCs: (a) Jute fibre grid bonding in FRGC (b) Bamboo fibre matrix in FRGC

Fig. 11 displays the outcomes of the variable (three point) bending investigation. The flexural reply of produced geopolymer composites clearly demonstrates impact of bamboo and jute fiber reinforcement. For both varieties of FRGCs, a continuous relation betwixt the fiber content and flexural strength was seen, in contrast to the findings of the compression and splitting tensile tests (Fig. 11a and b). With a fiber percentage of 2% (wt.%), Jute FRGCs had the higher flexural strength of 3.3 MPa, which is 329% greater than the control matrix. According to studies by (Sun *et al.* 2008; Chen *et al.* 2014), it has been suggested that the fibbers' assistance in carrying greater tensile stresses across cracks accounts for the gain in flexural strength seen in FRGCs. Figures 11s, respectively, depict the failure posture of the control matrix, 3% FRGC jute and 4% bamboo-FRGC at the final case. When exhibit is reinforced with fibers, the inclusion of both fibers significantly alters the failure behaviour, changing it from a sudden, brittle crack to a composed, further adhesive failure. The displacement curve (Fig. 11c) demonstrated that control matrix of flexural modulus and FRFGs. It has been demonstrated that the behaviour of mechanical of FRGCs was composed by the geopolymer matrix's structure as well as the kind and quantity of natural fibers (Ardanuy *et al.* 2015; Thirumalvalavan *et al.* 2023). Jute and bamboo fibers exhibit strong adhesion to the FCBP-based geopolymer matrix, as evidenced by the SEM images presented in Figures 12a and 12b, respectively.

4. CONCLUSIONS

Geopolymer based on powdered natural fiber reinforced burned clay bricks has been developed as a possible building material with good mechanical qualities and minimal environmental impact. Geopolymers manufactured from brick wastes exhibited improved mechanical behaviour when combined with short jute and bamboo fibers. The raw and hard characteristics of the geopolymer composites fiber reinforced depend on the kind and quantity of fibers combined with FCBP. When compared to the matrix of

control (FCBP base geopolymer which is unreinforced), fiber content which is derived from jute FRGC with 1.5 % by weight demonstrated biggest improvement in tensile and compressive strengths at 64% and 45%, respectively. When compared to the matrix of control, bamboo-FRGCs performed best at a 2.5% (wt.%) fiber content, improving the tensile strength by 112% and the compressive strength by 76%. All of strain and stress curves and the specimens' failure condition showed that the inclusion of fibers encouraged reinforced samples. A continuous link among the flexural strength and natural fibre of FRGC was revealed by three-point bending tests. With 2% content of fiber the flexural strength of FRGC jute was 3.3 MPa which is equivalent to a 329% increase over the unreinforced matrix. Like this, bamboo-FRGCs outperformed unreinforced FCBP-based geopolymer, exhibiting a 3.5 MPa flexural strength at 3% fiber content (a 360% improvement).

FUNDING

This research received no specific grant from any funding agency in the public, commercial, or not-for-profit sectors.

CONFLICTS OF INTEREST

The authors declare that there is no conflict of interest.

COPYRIGHT

This article is an open-access article distributed under the terms and conditions of the Creative Commons Attribution (CC BY) license (<http://creativecommons.org/licenses/by/4.0/>).



REFERENCES

- Alomayri, T., Shaikh, F. U. A., Low, I. M., Characterisation of cotton fibre-reinforced geopolymer composites, *Compos. Part B Eng.* 50, 1–6 (2013).
<https://doi.org/10.1016/J.COMPOSITESB.2013.01.013>
- Ardanuy, M., Claramunt, J., Toledo Filho, R. D., Cellulosic fiber reinforced cement-based composites: A review of recent research, *Constr. Build. Mater.* 79, 115–128 (2015).
<https://doi.org/10.1016/J.CONBUILDMAT.2015.01.035>
- Arisoy, B., Wu, H. C., Material characteristics of high performance lightweight concrete reinforced with PVA, *Constr. Build. Mater.* 22(4), 635–645 (2008).
<https://doi.org/10.1016/J.CONBUILDMAT.2006.10.010>
- Atiş, C. D., Görür, E. B., Karahan, O., Bilim, C., Ilkentapar, S., Luga, E., Very high strength (120 MPa) class F fly ash geopolymer mortar activated at different NaOH amount, heat curing temperature and heat curing duration, *Constr. Build. Mater.* 96, 673–678 (2015).
<https://doi.org/10.1016/J.CONBUILDMAT.2015.08.089>
- Bledzki, A. K., Franciszczak, P., Osman, Z., Elbadawi, M., Polypropylene biocomposites reinforced with softwood, abaca, jute, and kenaf fibers, *Ind. Crops Prod.* 70, 91–99 (2015).
<https://doi.org/10.1016/J.INDCROP.2015.03.013>
- Chen, C. H., Chen, C. Y., Lo, Y. W., Mao, C. F., Liao, W. T., Characterization of alkali-treated jute fibers for physical and mechanical properties, *J. Appl. Polym. Sci.* 80(7), 1013–1020 (2001).
<https://doi.org/10.1002/APP.1184>
- Chen, R., Ahmari, S., Zhang, L., Utilization of sweet sorghum fiber to reinforce fly ash-based geopolymer, *J. Mater. Sci.* 49(6), 2548–2558 (2014).
<https://doi.org/10.1007/S10853-013-7950-0/METRICS>
- Cheng, T. W., Chiu, J. P., Fire-resistant geopolymer produced by granulated blast furnace slag, *Miner. Eng.* 16(3), 205–210 (2003).
[https://doi.org/10.1016/S0892-6875\(03\)00008-6](https://doi.org/10.1016/S0892-6875(03)00008-6)
- Correia, E. A. S., Torres, S. M., de Oliveira Alexandre, M. E., Gomes, K. C., P. Barbosa, N., de Barros, S. R., Mechanical Performance of Natural Fibers Reinforced Geopolymer Composites, *Mater. Sci. Forum* 758, 139–145 (2013).
<https://doi.org/10.4028/www.scientific.net/MSF.758.139>
- Deepanraj, B., Thirumalvalavan, S., Selvarasu, S., Senthilkumar, N., Shaik, F., Investigation and optimization of wear properties of flax fiber reinforced Delrin polymer composite, *Mater Today Proc.* (2023).
<https://doi.org/10.1016/J.MATPR.2023.03.173>
- Dhinakarraj, C. K., Senthilkumar, N., Palanikumar, K., Deepanraj, B., Experimental interrogations on morphologies and mechanical delineation of silicon nitride fortified Mg-Al-Zn alloy composites, *Mater. Today Commun.* 35, 105731 (2023).
<https://doi.org/10.1016/J.MTCOMM.2023.105731>
- Dias, D. P., Thaumaturgo, C., Fracture toughness of geopolymeric concretes reinforced with basalt fibers, *Cem. Concr. Compos.* 27(1), 49–54 (2005).
<https://doi.org/10.1016/J.CEMCONCOMP.2004.02.044>
- Ghosh, S. K., Ghosh, S. K., Construction and Demolition Waste, *Sustain. Solid Waste Manag.* , 511–547 (2016).
<https://doi.org/10.1061/9780784414101.CH16>
- Korniejenko, K., Frączek, E., Pytlak, E., Adamski, M., Mechanical Properties of Geopolymer Composites Reinforced with Natural Fibers, *Procedia Eng.* 151, 388–393 (2016).
<https://doi.org/10.1016/J.PROENG.2016.07.395>
- Li, W., Xu, J., Impact characterization of basalt fiber reinforced geopolymeric concrete using a 100-mm-diameter split Hopkinson pressure bar, *Mater. Sci. Eng. A* 513–514(C), 145–153 (2009).
<https://doi.org/10.1016/J.MSEA.2009.02.033>
- Li, Y., Mai, Y. W., Ye, L., Sisal fibre and its composites: a review of recent developments, *Compos. Sci. Technol.* 60(11), 2037–2055 (2000).
[https://doi.org/10.1016/S0266-3538\(00\)00101-9](https://doi.org/10.1016/S0266-3538(00)00101-9)
- Mo, B. H., Zhu, H., Cui, X. M., He, Y., Gong, S. Y., Effect of curing temperature on geopolymerization of metakaolin-based geopolymers, *Appl. Clay Sci.* 99, 144–148 (2014).
<https://doi.org/10.1016/J.CLAY.2014.06.024>
- Natali, A., Manzi, S., Bignozzi, M. C., Novel fiber-reinforced composite materials based on sustainable geopolymer matrix, *Procedia Eng.* 21, 1124–1131 (2011).
<https://doi.org/10.1016/J.PROENG.2011.11.2120>
- Pacheco-Torgal, F., Castro-Gomes, J. P., Jalali, S., Investigations of tungsten mine waste geopolymeric binder: Strength and microstructure, *Constr. Build. Mater.* 22(11), 2212–2219 (2008).
<https://doi.org/10.1016/J.CONBUILDMAT.2007.08.003>
- Pacheco-Torgal, F., Jalali, S., Influence of sodium carbonate addition on the thermal reactivity of tungsten mine waste mud based binders, *Constr. Build. Mater.* 24(1), 56–60 (2010).
<https://doi.org/10.1016/J.CONBUILDMAT.2009.08.018>
- Phologolo, T., Yu, C., Mwasiagi, J. I., Muya, N., Li, Z. F., Production and Characterization of Kenyan Sisal, *Asian J. Text.* 2(2), 17–25 (2012).
<https://doi.org/10.3923/AJT.2012.17.25>
- Puertas, F., Amat, T., Fernández-Jiménez, A., Vázquez, T., Mechanical and durable behaviour of alkaline cement mortars reinforced with polypropylene fibres, *Cem. Concr. Res.* 33(12), 2031–2036 (2003).
[https://doi.org/10.1016/S0008-8846\(03\)00222-9](https://doi.org/10.1016/S0008-8846(03)00222-9)
- Ramu, S., Senthilkumar, N., Deepanraj, B., Mechanical characterization of E-glass fiber/aluminium powder filled with and without coconut fiber reinforced epoxy hybrid composite, *Mater Today Proc.* (2023).
<https://doi.org/10.1016/J.MATPR.2023.03.074>

- Ranjbar, N., Talebian, S., Mehrali, M., Kuenzel, C., Cornelis Metselaar, H. S., Jumaat, M. Z., Mechanisms of interfacial bond in steel and polypropylene fiber reinforced geopolymer composites, *Compos. Sci. Technol.* 122, 73–81 (2016).
<https://doi.org/10.1016/J.COMPSCITECH.2015.11.009>
- Reig, L., Tashima, M. M., Borrachero, M. V., Monzó, J., Cheeseman, C. R., Payá, J., Properties and microstructure of alkali-activated red clay brick waste, *Constr. Build. Mater.* 43, 98–106 (2013a).
<https://doi.org/10.1016/J.CONBUILDMAT.2013.01.031>
- Reig, L., Tashima, M. M., Soriano, L., Borrachero, M. V., Monzó, J., Payá, J., Alkaline activation of ceramic waste materials, *Waste and Biomass Valorization* 4(4), 729–736 (2013b).
<https://doi.org/10.1007/S12649-013-9197-Z/METRICS>
- Sá Ribeiro, R. A., Sá Ribeiro, M. G., Sankar, K., Kriven, W. M., Geopolymer-bamboo composite – A novel sustainable construction material, *Constr. Build. Mater.* 123, 501–507 (2016).
<https://doi.org/10.1016/J.CONBUILDMAT.2016.07.037>
- Silva, F. de A., Filho, R. D. T., Filho, J. de A. M., Fairbairn, E. de M. R., Physical and mechanical properties of durable sisal fiber–cement composites, *Constr. Build. Mater.* 24(5), 777–785 (2010).
<https://doi.org/10.1016/J.CONBUILDMAT.2009.10.030>
- Silva, G., Castañeda, D., Kim, S., Castañeda, A., Bertolotti, B., Ortega-San-Martin, L., Nakamatsu, J., Aguilar, R., Analysis of the production conditions of geopolymer matrices from natural pozzolana and fired clay brick wastes, *Constr. Build. Mater.* 215, 633–643 (2019).
<https://doi.org/10.1016/J.CONBUILDMAT.2019.04.247>
- Silva, G., Kim, S., Aguilar, R., Nakamatsu, J., Natural fibers as reinforcement additives for geopolymers – A review of potential eco-friendly applications to the construction industry, *Sustain. Mater. Technol.* 23, e00132 (2020a).
<https://doi.org/10.1016/J.SUSMAT.2019.E00132>
- Silva, G., Kim, S., Bertolotti, B., Nakamatsu, J., Aguilar, R., Optimization of a reinforced geopolymer composite using natural fibers and construction wastes, *Constr. Build. Mater.* 258, 119697 (2020b).
<https://doi.org/10.1016/J.CONBUILDMAT.2020.119697>
- Sun, P., Wu, H. C., Transition from brittle to ductile behavior of fly ash using PVA fibers, *Cem. Concr. Compos.* 30(1), 29–36 (2008).
<https://doi.org/10.1016/J.CEMCONCOMP.2007.05.008>
- Thirumalvalavan, S., Senthilkumar, N., Deepanraj, B., Syam Sundar, L., Assessment of mechanical properties of flax fiber reinforced with Delrin polymer composite, *Mater Today Proc.*
<https://doi.org/10.1016/J.MATPR.2023.03.087>
- Yan, L., Chouw, N., Behavior and analytical modeling of natural flax fibre-reinforced polymer tube confined plain concrete and coir fibre-reinforced concrete, *Journal of Composite Materials*, 47(17), 2133–2148 (2012).
<https://doi.org/10.1177/0021998312454691>
- Yazıcı, Ş., Inan, G., Tabak, V., Effect of aspect ratio and volume fraction of steel fiber on the mechanical properties of SFRC, *Constr. Build. Mater.* 21(6), 1250–1253 (2007).
<https://doi.org/10.1016/J.CONBUILDMAT.2006.05.025>
- Zhao, Q., Nair, B., Rahimian, T., Balaguru, P., Novel geopolymer based composites with enhanced ductility, *J. Mater. Sci.* 42(9), 3131–3137 (2007).
<https://doi.org/10.1007/S10853-006-0527-4/METRICS>